

Focal Accumulation of Iodine-123-BMIPP in Liposarcoma of the Thigh

Y. Suto, Y. Tanabe and Y. Ohta

Department of Radiology, Tottori University Faculty of Medicine, Nishimachi, Yonago, Japan

Findings for focal accumulation of ^{123}I -15-(*p*-iodophenyl)-3-*R,S*-methylpentadecanoic acid (^{123}I BMIPP) in a patient with liposarcoma of the thigh are presented. Iodine-123-BMIPP accumulated heterogeneously in the liposarcoma. The region with marked accumulation of ^{123}I BMIPP was diagnosed as mixoid liposarcoma. The region with little accumulation of ^{123}I BMIPP was diagnosed as well-differentiated liposarcoma. Differences in the accumulation of ^{123}I BMIPP may reflect differences in fatty acid metabolism between histopathological types of liposarcoma.

Key Words: iodine-123-BMIPP; liposarcoma; fatty acid metabolism; tumor imaging

J Nucl Med 1996; 37:997-999

Iodine-123-15-(*p*-iodophenyl)-3-*R,S*-methylpentadecanoic acid (^{123}I BMIPP) is a radioactive agent developed for evaluation of local fatty acid metabolism in cardiac muscle. To date, clinical studies with this drug have been limited for the most part to the area of the heart. In this report, we present interesting findings for a patient with liposarcoma of the thigh which exhibited focal accumulation of ^{123}I BMIPP.

CASE REPORT

A 41-yr-old man noticed swelling (a 4–5-cm tumor) on the frontal aspect of the right thigh about 1 yr earlier. Since no significant pain was felt, the patient left the tumor untreated for some time. Later, the tumor began gradually to grow, and the patient experienced marked pain at the tumor site and was admitted to our hospital. The tumor measured 135 × 115 × 50 mm at the time of admission. The tumor was multilobular, soft and elastic.

Neither heat nor rubor was noted on the surface of the tumor. Adhesion of the tumor to nearby skin and muscle was noted. No abnormalities were observed on blood biochemical testing or urinalysis, and no tumor markers were detected in the blood. We assumed that some changes in fatty acid metabolism might occur in tumor tissues of patients and that ^{123}I BMIPP accumulation might be different in tumor tissues compared with that in normal tissue. The details of the examination were explained to the patient who then gave informed consent to undergo ^{123}I BMIPP scintigraphy.

After fasting for more than 2 hr, the patient was administered 111 MBq ^{123}I BMIPP intravenously. At 30 min and 3 hr after injection, planar images of the front and lateral views of the thoracoabdominal and right femoral regions were obtained. Imaging was performed with a 20% window centering on 159 keV, and each scintigram was obtained at 600K cts. Images were obtained with a gamma camera equipped with medium-energy collimation.

Thirty minutes postinjection, ^{123}I BMIPP accumulation in the femoral tumor was heterogenous: accumulation in the tumor was generally less than that in the muscle but was denser than that in the muscle in one region inside the tumor (Fig. 1). No abnormal

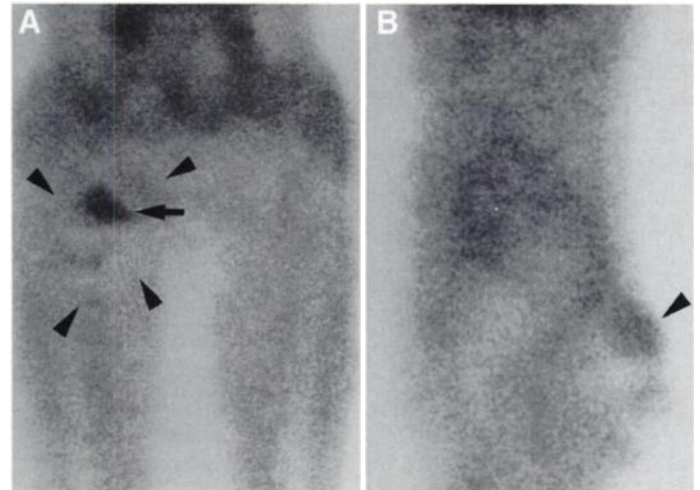


FIGURE 1. Scintigrams obtained 30 min after intravenous injection of ^{123}I BMIPP. (A) Anterior view of the right thigh. (B) Lateral view of the same region as in A. The giant tumor (arrowheads) on the frontal aspect of the right thigh generally exhibited less accumulation than the surrounding muscles, but a region (arrow) accumulating more radioactivity than muscle was found inside the tumor.

accumulation was detected in the thoracoabdominal region. Similar images were obtained 3 hr postinjection.

Three days before ^{123}I BMIPP scintigraphy, ^{201}Tl scans were obtained twice. Early phase scintigraphy was performed 15 min after the intravenous injection of 74 MBq ^{201}Tl -Cl. Late phase images were obtained 4 hr later. Both ^{201}Tl images revealed no abnormal accumulation to the tumor (Fig. 2).

Two days after ^{123}I BMIPP scintigraphy, magnetic resonance (MR) images were obtained with a 1.5 Tesla superconducting system. T1-weighted images (T1WI; TR msec/TE msec/signal averages = 600/22/3) and T2-weighted images (T2WI; 2000/90/2) were obtained. MRI demonstrated heterogenous appearance of the tumor which was separated into two signal components: one region exhibited lower signal intensities than hypodermal fat on T1WI, higher signal intensities than hypodermal fat on T2WI, while the other region exhibited high signals similar to those of hypodermal fat on T1WI and T2WI (Fig. 3). A comparison of the MR images and ^{123}I BMIPP scintigram revealed that the former region correlated with that exhibiting marked accumulation of ^{123}I BMIPP and the latter with the region of slight ^{123}I BMIPP accumulation.

The patient then underwent 30-Gy ^{60}Co irradiation followed by surgical extraction of the tumor. The size of the excised tumor was 120 × 115 × 40 mm. After comparative examination of gross findings on extracted specimen and the ^{123}I BMIPP scans, the area with obvious accumulation of BMIPP and that with less accumulation were examined histologically. The tumor was histologically diagnosed as liposarcoma. Its internal structure was heterogenous and the region with ^{123}I BMIPP accumulation was identified as

Received Jul. 6, 1995; revision accepted Sept. 7, 1995.

For correspondence or reprints contact: Yuji Suto, MD, Department of Radiology, Tottori University Faculty of Medicine, 36-1 Nishimachi, Yonago 683, Japan.

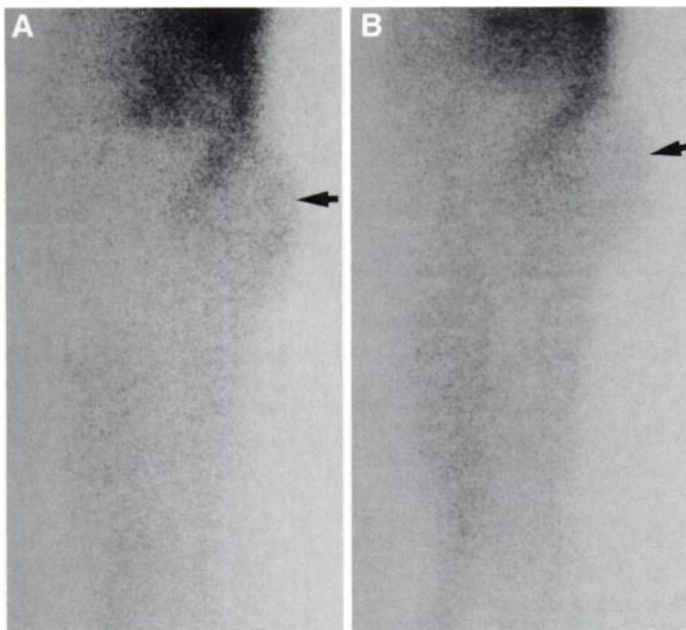


FIGURE 2. Lateral view of ^{201}Tl images. (A) Early phase image. (B) Late phase image. Both images revealed no abnormal accumulation in the tumor (arrow).

mixoid liposarcoma. The region with little accumulation of [^{123}I]BMIPP was identified as well-differentiated liposarcoma.

DISCUSSION

In various experimentally induced tumors in animals, accelerated transport of fatty acids into tumors (1,2), accelerated oxidation of fatty acids as metabolic fuel in tumor cells (3) and accelerated lipid metabolism in tumors for the synthesis of membrane-related lipid complexes (4) have been observed. Current clinical studies with [^{123}I]BMIPP, however, have been limited to the myocardium.

In their study in animal models, Kubota et al. (5) attempted to detect various tumors using radiolabeled fatty acids including [^{123}I]BMIPP. They concluded that labeled fatty acids were not useful for detecting tumors, but no liposarcomas were included in their study.

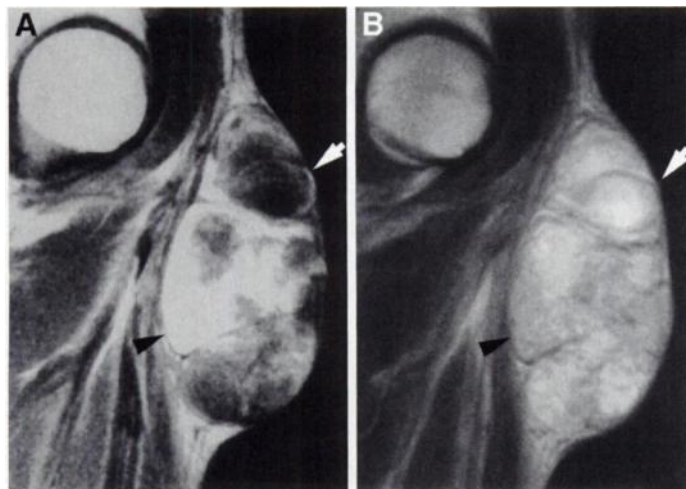


FIGURE 3. MR images. (A) T1-weighted image (T1WI) (TR/TE/signal averagings = 600 msec/22 msec/3). (B) T2-weighted image (T2WI) (2000/90/2). Inside the giant tumor, signal intensities were separated into two main components. One region (arrow) exhibited lower signal intensities than fat on T1WI as well as higher signal intensities than fat on T2WI, while the other (arrowhead) exhibited high signal intensity similar to those of fat on T1WI and T2WI.

After intravenous injection, [^{123}I]BMIPP rapidly disappears from the blood and accumulates in myocardium and liver, where fatty acid metabolism occurs rapidly (6). Accumulation in muscles is slight and diffuse, and accumulation in organs other than the liver and heart is extremely low (6). According to Kubota et al. (5), the ratio of accumulation of [^{123}I]BMIPP in tumor to that in muscle was 1 or higher from 30 min after intravenous injection onwards in a rat hepatoma model that had been subcutaneously transplanted.

In the present study, images were obtained not only 30 min (early phase) but also 3 hr (late phase) after intravenous injection. At these two time points, similar heterogeneous [^{123}I]BMIPP accumulation was observed. The ^{201}Tl scans, however, did not reveal significant accumulation. The mechanism of tumoral ^{201}Tl uptake is probably dependent on both blood flow and permeability of ^{201}Tl through the cell membranes (7). Various reports have shown a discrepant distribution of [^{123}I]BMIPP from ^{201}Tl in ischemic heart diseases (8) and in cardiomyopathy (9). These data indicate that BMIPP distribution may reflect metabolic alterations rather than mere perfusion in various abnormal conditions (8).

Liposarcoma is one of the more common malignant soft-tissue tumors. This tumor consists of admixtures of fat cells and soft-tissue components in varying proportion (10). It has been reported that signal intensity in MRI inside liposarcoma differ by histologic type, that mixoid liposarcoma exhibited lower signal intensities than hypodermal fat on T1WI and higher signal intensities than hypodermal fat on T2WI, and that well-differentiated liposarcoma had high signal intensities similar to those of hypodermal fat on T1WI and T2WI (11-13). These findings are similar to those obtained in the present study.

In our comparison of [^{123}I]BMIPP accumulation with histological findings, accumulation of [^{123}I]BMIPP in the region of well-differentiated liposarcoma was found to be less than that in the surrounding muscle, while the region of mixoid liposarcoma corresponded to the region of marked accumulation of [^{123}I]BMIPP. Although the reasons for this difference in [^{123}I]BMIPP distribution are not yet known in detail, this difference may reflect differences in fatty acid metabolism between the histologic types included in this tumor. Difference in cell densities, higher cell density in the mixoid and lower cell density and large fat in the well-differentiated tumor, might be factors related to [^{123}I]BMIPP accumulation.

Our findings are of particular interest in that intratumoral fatty acid metabolism, which had previously only been used in PET studies, was visualized using a single-photon imaging agent.

Visualization of fatty acid metabolism in tumors might aid in the diagnosis of tumors and observation of their clinical course. Further studies will be required to establish the clinical usefulness of our method.

ACKNOWLEDGMENT

We thank Nihon Medi-Physics Co., Ltd for supplying the [^{123}I]BMIPP.

REFERENCES

- Mermier P, Baker N. Flux of free fatty acids among host tissues, ascites fluid and Ehrlich ascites carcinoma cells. *J Lipid Res* 1974;15:339-351.
- Stremmel W, Diede HE. Fatty cell lines represent a carrier-mediated uptake process. *Biochem Biophys Acta* 1989;1013:218-222.
- Ookhtens M, Baker N. Fatty acid oxidation to H_2O by Ehrlich carcinoma in mice. *Cancer Res* 1979;39:973-980.
- Wiegand RD, Wood R. Lipids of cultured hepatoma cells: III. triglyceride and phosphoglyceride biosynthesis in minimal deviation hepatoma 7288C. *Lipid* 1974;9:141-148.
- Kubota K, Takahashi T, Fujiwara T, et al. Possibility for tumor detection with fatty acid analogs. *Nucl Med Biol* 1991;18:191-195.
- Torizuka K, Yonekura Y, Nishimura T, et al. The phase one study of β -methyl- ^{123}I -iodophenyl-pentadecanoic acid. *Jpn J Nucl Med* 1991;28:681-690.

7. Terui S, Terauchi T, Abe H, et al. On clinical usefulness of ^{201}Tl scintigraphy for the management of malignant soft-tissue tumors. *Ann Nucl Med* 1994;8:55-64.
8. Tamaki N, Kawamoto Y, Yonekura Y, et al. Regional metabolic abnormality in relation to perfusion and wall motion in patients with myocardial infarction: assessment with emission tomography using an iodinated branched fatty acid analog. *J Nucl Med* 1992;33:659-667.
9. Kurata C, Kobayashi A, Yamazaki N. Dual-tracer autoradiographic study with thallium-201 and radioiodinated fatty acid in cardiomyopathic hamsters. *J Nucl Med* 1989;30:80-87.
10. Scott WW Jr, Fishman EK. Soft-tissue masses. In: Scott WW Jr, Magid D, Fishman EK, eds. *Computed tomography of the musculoskeletal system*. New York: Churchill Livingstone;1987:1-27.
11. London J, Kim EE, Wallace S, Shirhoda A, Coan J, Evans H. MR imaging of liposarcomas: correlation of MR features and histology. *J Comput Assist Tomogr* 1989;13:832-835.
12. Sundaram M, Baran G, Merenda G, et al. Mixoid liposarcoma: magnetic resonance imaging appearance with clinical and histological correlation. *Skel Radiol* 1990;19:359-362.
13. Harms SE, Greenway G. Musculoskeletal system. In: Stark DD, Bradley WG Jr, eds. *Magnetic resonance imaging*, 2nd ed, vol. 2. St. Louis: Mosby; 1992:2107-2222.

Bone Metastasis with Superimposed Osteomyelitis in Prostate Cancer

Martha Pruckmayer, Christoph Glaser, Christian Nasel, Susanna Lang, Michael Rasse and Thomas Leitha
University Clinics of Nuclear Medicine, Maxillofacial Surgery, Radiology and Clinical Pathology, Vienna, Austria

The following case of a male patient with a history of prostate cancer suffering from pain and swelling in the right mandibular area illustrates the well-known diagnostic problem of a superinfected tumor. Orthopan tomography and CT showed no defects in bone structure or smooth tissue. Whole-body bone scanning showed increased tracer uptake in the mandibular bone and in several other locations in the skeletal system. Antigranulocyte immunoscintigraphy showed increased uptake over the right mandible, whereas the other metastatic sites were visualized as cold spots. A second CT scan depicted a sclerotic lesion with surrounding periosteal reaction and soft-tissue swelling and was interpreted as osteomyelitis. Therefore, clinical symptoms, bone scanning, antigranulocyte immunoscintigraphy and follow-up CT resulted in a diagnosis of osteomyelitis, although open needle biopsy revealed the lesion to be prostate cancer metastasis with massive leukocytic invasion.

Key Words: antigranulocyte immunoscintigraphy; prostate cancer; bone metastases; SPECT

J Nucl Med 1996; 37:999-1001

Antigranulocyte immunoscintigraphy has been validated for the specific diagnosis and localization of focal granulocytic infections (1-3). The monoclonal antibody (MAb) 250/183 is a murine monoclonal Ig G1 antibody. It is directed against CEA nonspecific cross-reacting antigen (NC-95) exposed at the cellular membrane of peripheral granulocytes and myelocytes (4). About 80% of these are located in bone marrow (5). Two to 6 hr after administration, the labeled antibody normally accumulates in the liver, spleen and bone marrow (6). Its utility in detecting bone infection has been demonstrated (1,2,7-11).

In cancer patients, MAb 250/183 is utilized for bone marrow scanning. It indirectly visualizes the replacement of hematopoietic tissue in the bone marrow cavity by bone metastases as cold lesions (12). In contrast, bone scintigraphy visualizes osteoblastic metastases as hot spots due to the focal increase of osteoblastic activity. Thus, both diagnostic imaging procedures are used complementarily to image bone metastases (13-15), yet show similar tracer enhancement in osteomyelitis.

These concepts appeared feasible for application in the differential diagnosis of metastatic bone disease and osteomyelitis. In this report, we discuss the limitations of several



FIGURE 1. Orthopan tomography shows no sign of malignant destruction of the osseous structure in the right mandible.

imaging modalities in a case of metastatic tumor disease and superimposed osteomyelitis in the mandible.

CASE REPORT

A 62-yr-old man with a history of prostate cancer was examined because of progressive pain and swelling of the right mandibular region. Orthopan tomography showed no defects in bone structure in the mandibular region (Fig. 1). CT scans depicted no osteodestruction and thus appeared to be compatible with acute osteomyelitis.

Whole-body bone scintigraphy (3 hr postinjection of 600 MBq $^{99\text{m}}\text{Tc}$ -diphosphonate) indicated multiple sites of increased tracer uptake in several locations of the skeletal system, a phenomenon compatible with advanced metastatic disease (Fig. 2A). The local scintigram of the cranium showed increased tracer uptake over nearly the whole corpus of the right mandible. Because differential diagnosis between osteomyelitis and neoplastic lesions is not possible in static bone imaging alone, antigranulocyte immunoscintigraphy was recommended.

Bone scans and immunoscintigrams with MAb 250/183 were acquired with a double-headed gamma camera fitted with a low-energy, high-resolution, parallel-hole collimator (about 700,000 total counts). Antigranulocyte whole-body immunoscintigraphy was performed 6 hr after administration of 300 MBq radiolabeled BW 250/183. It showed typical cold lesions at the sites of hot spots on the bone scan, again consistent with the scintigraphic equivalent for metastatic marrow replacement (Fig. 2B). The mandibular hot spot on the bone scan was the only

Received Jul. 6, 1995; revision accepted Sept. 12, 1995.

For correspondence or reprints contact: Martha Pruckmayer, MD, University Clinic of Nuclear Medicine, General Hospital Vienna, Leitstelle 3L, Waehringer Guertel 18-20, A-1090 Vienna, Austria.